Calibration and Reliability in Groundwater Modelling: From Uncertainty to Decision Making
(Proceedings of ModelCARE'2005, The Hague, The Netherlands, June 2005). IAHS Publ. 304, 2006.

Recharge fronts and stagnation areas for pumping wells

M. RIVA & A. GUADAGNINI
Politecnico di Milano, D.I.I.A.R., Piazza Leonardo da Vinci 32, I-20133 Milano, Italy
monica.riva@polimi.it

Abstract We consider a single pumping well within a two-dimensional heterogeneous aquifer, in the presence of a mean uniform background gradient. We analyse the uncertainty associated with the location of the stagnation point which is generated downstream of the well and the maximum lateral extent of the well recharge area. The study is relevant for risk assessment practice, since it allows one to estimate the maximum width of the region contributing to the well and to properly locate regions of inversion of the flow direction. The problem is approached within a numerical Monte Carlo framework and the dependence of the main statistics of the quantities of interest on the moments of the log-conductivity field is studied. An assessment of the impact of one conductivity datum at the pumping location is performed.
Keywords conditioning; stagnation point; stochastic; well-catchments; width of catchments

INTRODUCTION AND PROBLEM SETTING

Knowledge of the main characteristics of the region of influence of an extraction well operating in a (generally heterogeneous) aquifer is relevant for securing the long-term viability of drinking water derived from groundwater resources. A common way to cope with aquifer heterogeneity is to assume that the natural logarithm of the hydraulic conductivity is a Spatial Random Function, eventually conditioned upon measurements taken at some locations. This leads to a probabilistic interpretation of the concept of well catchment, which has been addressed both numerically, via Monte Carlo procedures (e.g. Franzetti & Guadagnini, 1996; Vassolo *et al*., 1998), and by means of analytical and semi-analytical methods (e.g. Stauffer *et al*., 2004; Riva *et al*., 2006).

Here we study the statistics of the main geometric features of the catchment of a pumping well which is extracting a given flow rate from a randomly heterogeneous aquifer. We are mainly concerned with the answer to the following key questions of practical interest: (a) what is our ability to predict the position of the stagnation point which is generated downstream of the well? and (b) what is our ability to predict the maximum width of the well catchment? While the location of the stagnation point is linked to the downstream limit of the region directly contributing water to the well, in standard practice the width of the well's region of influence is usually extended to the ultimate recharge area and is made to conform to variability in the mapped flow direction. To answer these questions, we consider the problem of a steady state pumping well located at the centre of a square domain, with the following boundary conditions: a prescribed hydraulic head is imposed on the west boundary, the north and south sides are impermeable, and a constant flux is imposed along the east boundary. We begin by studying the statistics of the stagnation point and maximum width of the well catchment as a function of the main statistics of the underlying log-conductivity field, in the presence of a deterministic and constant porosity. We then analyse the impact of one conductivity datum, K_m, available at the pumping station. This is a common situation in practice where the statistical properties of the hydraulic parameters of the aquifer can be (at best) inferred by pumping test analysis while the local conductivity at the well is generally inferred by sieve-analysis. The problem is tackled entirely within a numerical Monte Carlo framework.

DIMENSIONAL ANALYSIS

We set a Cartesian coordinate system, centred at the well, with the x-axis aligned along the direction of the mean background flow and oriented along the upstream direction. The stagnation point $\mathbf{x}_s \equiv (x_s, y_s)$ is described by the following functional relationship:

$$\mathbf{x}_s = f(K_c, Q, q_0, L) \tag{1}$$

where K_c is the (random) conditional conductivity process, Q is the well pumping rate per unit thickness of the aquifer, q_0 is the natural base flow, L is a characteristic length scale of the flow domain. Here and in the following f represents functional relationships at different stages of the dimensional analysis. We consider the case where a single measurement of conductivity, K_m, is available at the well position $\mathbf{x}_w \equiv (x_w, y_w)$. Then, the conditional log-conductivity, $Y_c = \ln K_c$, is expressed in terms of the unconditional and stationary log-conductivity field, Y, and the log-conductivity measured at the well, $Y_m = \ln K_m$. We model Y as a Gaussian process, characterized by its variance, σ_Y^2, correlation function (with correlation scale λ) and constant geometric mean of K, K_G; Q, q_0, and L are treated as deterministic quantities. It can be shown, on the basis of the work of Riva *et al*. (2006), that the first and second moment of a particle trajectory in a randomly heterogeneous medium do not depend (at least to second order—in σ_Y—of approximation) on K_G. For a given functional format of the log-conductivity covariance, the statistical moment of ith order of $\mathbf{x}_s$, $E[\mathbf{x}_s]^i$, is given by the relationship:

$$E[\mathbf{x}_s]^i = f(\lambda, K_m, \sigma_Y^2, Q, q_0, L) \tag{2}$$

Choosing Q and q_0 as fundamental quantities, the mean stagnation point, $\bar{\mathbf{x}}_s \equiv \bar{x}_s, \bar{y}_s$, is then given by:

$$\frac{\bar{x}_s}{x_{s0}} = f\left(\frac{\lambda}{L}, \frac{K_m}{q_0}, \sigma_Y^2, \frac{L}{Q/q_0}\right) \qquad \bar{y}_s = 0 \tag{3}$$

where x_{s0} is the abscissa of the stagnation point in a bounded, homogeneous aquifer. The longitudinal and transversal components of the variance of the stagnation point, which are respectively indicated as σ_{xs}^2 and σ_{ys}^2 are governed by:

$$\frac{\sigma_{xs}^2}{x_{s0}^2} = f\left(\frac{\lambda}{L}, \frac{K_m}{q_0}, \sigma_Y^2, \frac{L}{Q/q_0}\right) ; \qquad \frac{\sigma_{ys}^2}{(Q/q_0)^2} = f\left(\frac{\lambda}{L}, \frac{K_m}{q_0}, \sigma_Y^2, \frac{L}{Q/q_0}\right) \tag{4}$$

In our case the maximum transverse width of the catchment, D, occurs at the east side of the domain and is given by mass conservation as $D = Q/q_0$. Since Q and q_0 are deterministic, D is also constant and deterministic with a random location, y_G, of its centre of mass. Due to symmetry, the ensemble mean of y_G vanishes. The variance of y_G, σ^2_{yG}, is then provided by the following functional relationship:

$$\frac{\sigma^2_{yG}}{(Q/q_0)^2} = f\left(\frac{\lambda}{L}, \frac{K_m}{q_0}, \sigma^2_Y, \frac{L}{Q/q_0}\right) \tag{5}$$

Here we are concerned with heterogeneous domains with constant L, and boundary conditions (Q and q_0), so that the effects of $L/(Q/q_0)$ will not be considered in equations (3)–(5).

MODEL SIMULATION SET UP AND RESULTS

We performed numerical Monte Carlo simulations in a square domain discretized by 280×280 elements of uniform size $\Delta = 0.1$, in consistent units ($L = 280 \times \Delta = 28$). The constant hydraulic head $H = 10$ is prescribed along the west side, the constant flux $q_0 = 0.5$ (also in consistent units) is fixed along the east side; no-flow is imposed along the remaining sides. A well extracting the constant rate $Q = 4\pi q_0$ is placed at the centre of the grid ($x_w = 0$, $y_w = 0$). The Gaussian sequential simulator GCOSIM3D (Gómez-Hernández & Journel, 1993) was used to generate unconditional and conditional realizations of the log hydraulic conductivity with $K_G = 100$ and simple exponential covariance. The main parameters were varied within the following ranges: (i) $0.5 \le \lambda \le 30$ (i.e., $0.018 \le \lambda/L \le 1.071$), $0.1 \le \sigma^2_Y \le 1.0$ and $K_m = K_G$ (Test Case C1); (ii) $K_G \times \exp(2\sigma_Y)$ (Test Case C2); and (iii) $K_G \times \exp(-2\sigma_Y)$ (Test Case C3). A total of 1000 Monte Carlo runs were performed for each combination of parameters.

Figure 1 depicts the dependence of $\bar{x}_s / x_{s0}$ on λ/L and σ^2_Y for the unconditional (Fig. 1(a)) and conditional (Fig. 1(b)) scenarios. The 95% confidence intervals, rendering the uncertainty associated with the ensemble moment evaluated on the basis of a finite sample of Monte Carlo runs, are also reported for the unconditional results. In the unconditional case, we note that $\bar{x}_s / x_{s0}$ does not depend on the correlation scale when $\sigma^2_Y = 0.1$, and the largest percentage difference between $\bar{x}_s$ and x_{s0} is less than 3%. The effect of a finite correlation begins to appear for $\sigma^2_Y = 0.5$. The partial overlapping of the confidence intervals suggests that a quantitative analysis of the influence of λ/L and σ^2_Y on the mean stagnation point is not completely feasible with 1000 Monte Carlo runs. The results of Fig. 1(a) can be explained upon considering that the hydraulic conductivity is practically uncorrelated when λ/L is very small so that high and low conductivity blocks may alternate frequently in the domain; as a consequence, particle trajectories are characterized by frequent and small amplitude fluctuations around the mean. Contrariwise, when λ/L increases, the transport process is governed by contrasts of conductivities between large zones, so that particle trajectories can deviate significantly from the mean. The results reveal that the stagnation point is moved (in the mean) away from the well when λ/L is small. The

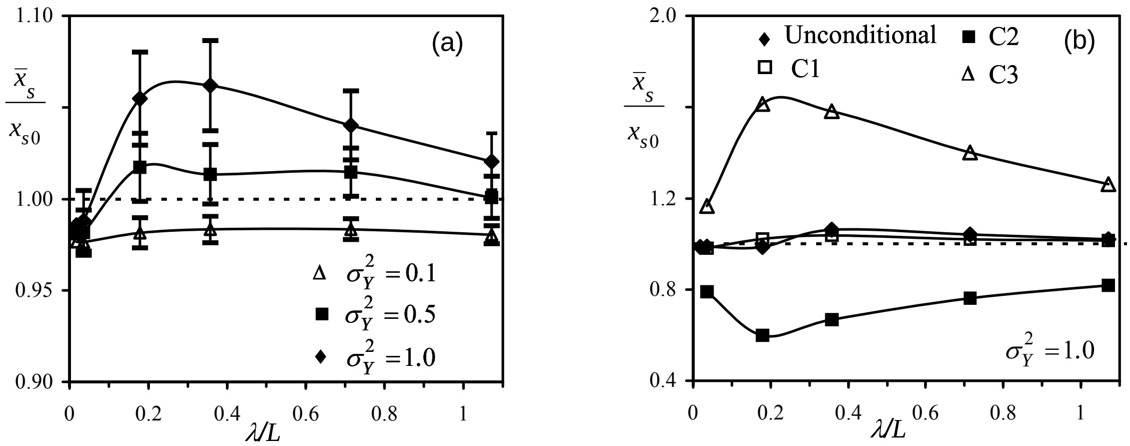

Fig. 1 Dependence of the normalized mean stagnation point on the normalized correlation scale for: (a) unconditional, and (b) conditional fields. Vertical bars indicate the 95% estimated confidence intervals.

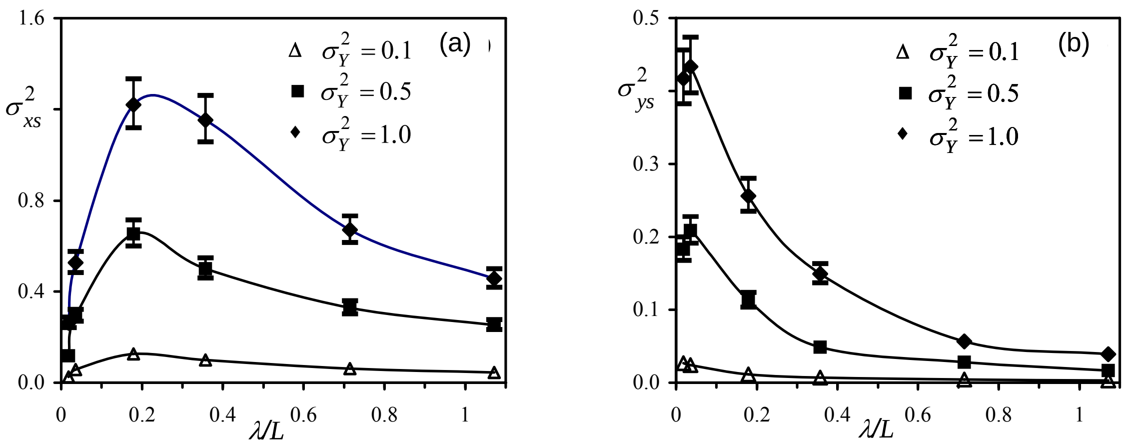

Fig. 2 Dependence of: (a) longitudinal, and (b) transverse variance of the stagnation point on λ/L and σ^2_Y for the unconditional cases. Vertical bars indicate the 95% estimated confidence intervals.

ratio $\bar{x}_s / x_{s0} \rightarrow 1$ when $\lambda/L \rightarrow \infty$, since hydraulic conductivity tends to become a random constant. In the conditional scenario (Fig. 1(b)) we note that $\bar{x}_s / x_{s0}$: (i) is not influenced by conditioning when $K_m = K_G$ (Test Case C1); and (ii) is located closer to or farther from the well if $K_m > K_G$ (Test Case C2) or $K_m < K_G$ (Test Case C3), respectively. While conditioning by large K_m forces solute particles to be attracted by the well, the opposite occurs when one conditions on low K_m. Similarly to what was observed previously, the behaviour is non-monotonic with λ/L.

Figure 2 depicts the dependence of the longitudinal (Fig. 2(a)) and transverse (Fig. 2(b)) variance of the stagnation point on λ/L and σ_Y^2, together with the associated 95% confidence intervals, for the unconditional simulations. Both variances first increase, reach a maximum and then decrease with λ/L. They vanish in the limits for $\lambda/L \rightarrow 0$ and $\lambda/L \rightarrow \infty$. This behaviour is explained by the same mechanism presented above. Our simulations reveal that both σ_{xs}^2 and σ_{ys}^2 increase linearly with σ_Y^2 (details not shown).

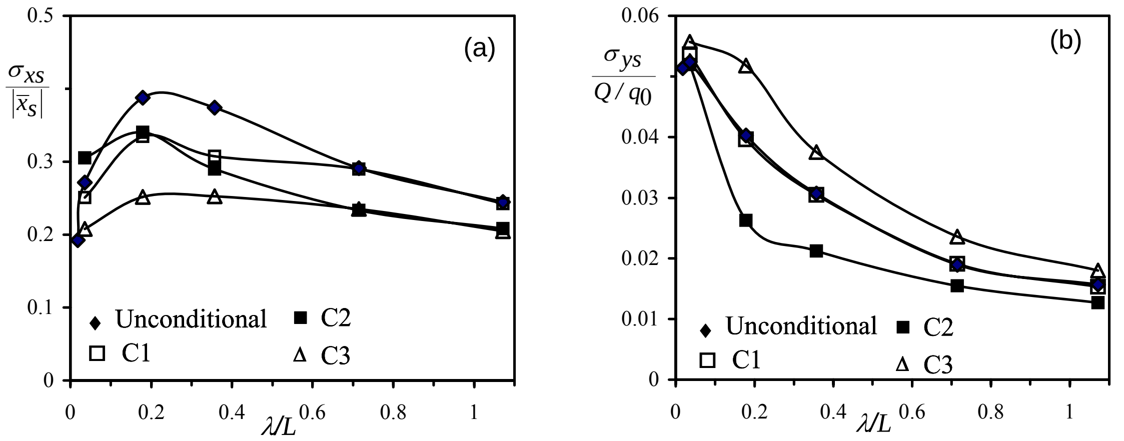

Fig. 3 Dependence of: (a) longitudinal, and (b) transverse dimensionless second order moments of the stagnation point on λ/L for the unconditional and conditional cases when $\sigma^2_Y = 1.0$.

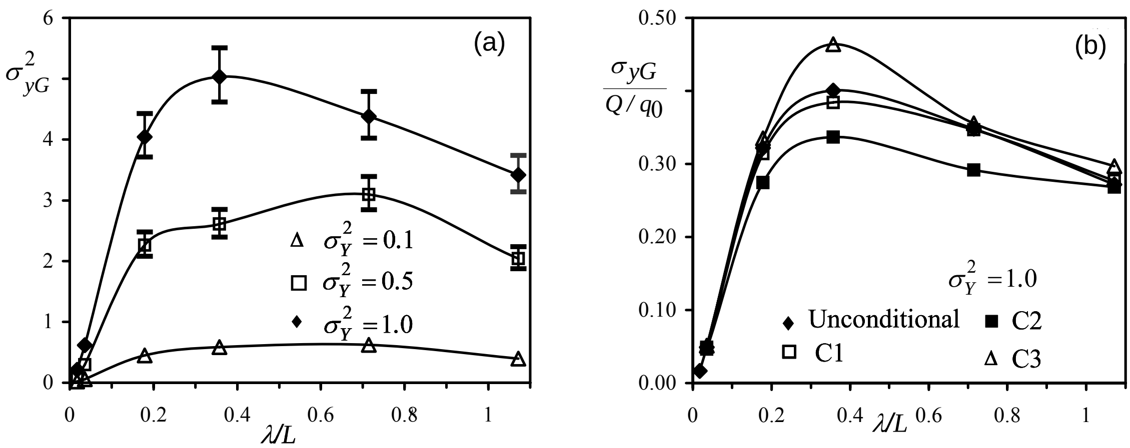

Fig. 4 (a) Dependence of the variance of y_G for the unconditional case on λ/L and σ^2_Y; and (b) dependence of standard deviation of y_G on λ/L for $\sigma^2_Y = 1.0$ for both unconditional and conditional cases. Vertical bars indicate the 95% estimated confidence intervals.

Figure 3 depicts the dependence of the dimensionless longitudinal, $\sigma_{xs} / |\bar{x}_s|$, and transverse, $\sigma_{ys}/(Q/q_0)$**,** standard deviations of the stagnation point for the unconditional and conditional cases, when $\sigma^2_Y = 1.0$. Figure 3(a) shows that conditioning generally produces a decrease of $\sigma_{xs} / |\bar{x}_s|$. The effect is stronger when conditioning is performed on the smallest K_m values, as the rate of increase of σ_{xs} with respect to λ/L is lower than that of the mean distance from the well, $|\bar{x}_s|$. For large values of λ/L conditioning on K_G has no effect, while conditioning on small or large K_m values has practically the same effect. In Fig. 3(b) one can recognize that $\sigma_{ys}/(Q/q_0)$ is practically not influenced by conditioning when $K_m = K_G$, while the uncertainty increases when conditioning is performed on low K_m values (the overall width of the region contributing to the well increases in the proximity of the well), and decreases for large K_m values (the overall transverse extent of the region of influence close to the well decreases).

Figure 4(a) depicts the unconditional variance of centre of gravity of the limit of the recharge front, σ^2_{yG}, as a function of λ/L and σ^2_Y, with the 95% confidence intervals. Similar to that observed for the variance of the stagnation point, increasing λ/L causes σ^2_{yG} to increase, to reach a maximum and finally to decrease. It appears that the value of λ/L at which σ^2_{yG} is maximum increases as σ^2_Y decreases. In contrast to what was observed for the stagnation point variance, σ^2_{yG} displays a nonlinear dependence on σ^2_Y, especially for large λ/L (not shown here). The dependence of the dimensionless second order moments of y_G, $\sigma_{yG} / (Q/q_0)$, on λ/L for the conditional and unconditional cases is depicted in Fig. 4(b) for $\sigma^2_Y = 1.0$. The effect of conditioning is similar to that observed for the transverse variance of the stagnation point.

CONCLUSIONS

Our work leads to the following major conclusions:

– The mean location of the stagnation point depends linearly on σ^2_Y, while it depends nonlinearly on λ/L. From a practical standpoint, the effect of λ/L and σ^2_Y is not very relevant (percentage differences between $\bar{x}_s$ and x_{s0} are less than 7% for all the cases considered), thus corroborating previous findings about robustness of the zero-order solution of low order moments of particle trajectories under non-uniform flow conditions (Riva *et al*., 2006). The mean stagnation point is drawn close to or far from the well, depending on whether the well is located within a locally high or low conductivity area. The predicted stagnation point practically coincides with that of a homogeneous domain when conductivity is highly correlated within the aquifer.

– Transverse and longitudinal variance of the stagnation point increase with σ^2_Y and display a non monotonic dependence on λ/L. Conditioning generally produces a decrease of the longitudinal coefficient of variation of the stagnation point. The uncertainty associated with the transverse location of the stagnation point is larger when the well is located within a locally low conductivity region.

– The dependence of the location of the centre of gravity of the well recharge front on the domain heterogeneity is qualitatively similar to what observed for the transverse variance of the stagnation point.

REFERENCES

Bear, J. & Jacobs, M. (1965) On the movement of water bodies injected into aquifers. *J. Hydrol.* **3**, 37–57.

Franzetti, S. & Guadagnini, A. (1996) Probabilistic estimation of well catchments in heterogeneous aquifers. *J. Hydrol.* **174**(1–2), 149–171.

Gómez-Hernández, J. J. & Journel, A. G. (1993) Joint sequential simulation of multi-Gaussian field. In: *Geostatistics Troia*'92, vol. 1 (ed. by A. Soares), 85–94. Kluwer Academic Publishers, Dordrecht, The Netherlands.

Riva, M., Guadagnini, A. & De Simoni, M. (2006) Assessment of uncertainty associated to the estimation of well catchments by moment equations. *Adv in Water Resour*. (in press).

Stauffer, F., Franssen, H. J. H. & Kinzelbach, W. (2004) Semi-analytical uncertainty estimation of well catchments: Conditioning by head and transmissivity data. *Water Resour. Res*. **40**, W08305, doi:10.1029/2004WR003320.

Vassolo, S, Kinzelbach, W. & Schäfer, W. (1998) Determination of well head protection zone by stochastic inverse modeling. *J. Hydrol.* **206** (3/4), 268–280.